

Scattering Components from Low Grazing Angle Sea Clutter

T Lamont-Smith, P W Shepherd* and M R Gates

QinetiQ, Lovell Building, St Andrew's Road, Malvern, Worcs, WR14 3PS

* TW Research, Harcourt Barn, Harcourt Lane, Malvern, Worcs, WR14 4DW

Abstract

Doppler spectra of low grazing angle sea clutter have been examined and two different, slow and fast, scattering components have been identified and modelled. Trends in real radar data with different parameters have been empirically identified. A statistical model based on two Gaussian spectral components has been developed, and its performance assessed in comparison to real data. A method of simulation using a memoryless non-linear transform has also been developed.

Keywords: EM scattering, low grazing angle, Doppler

Introduction

Bragg scattering was first proposed as an important scattering mechanism for radar backscatter from the sea surface by Crombie [1]. The frequency of the peak in the Doppler spectrum was consistent with the phase velocity of the swell waves that were Bragg-resonant at that wavelength (decametre). At short radar wavelengths, Bragg resonance has also been the dominant paradigm used in describing scattering from the sea surface. Two-scale composite scattering theory has formed the basis of much of the theoretical modelling work on scattering from the sea surface with Bragg resonant ripples tilted by longer wavelength gravity waves.

It has been observed that at low grazing angles the HH polarised return from the sea surface has a significantly larger peak Doppler frequency than VV [2], which has proven difficult to explain by composite scattering theory. Plant [3] has recently developed a Bragg scattering model that can resolve this discrepancy by assuming the presence of bound centimetric waves on the front of the steep waves. In contrast, a number of authors have recognised that non-Bragg scattering is important, and is

generally associated with wave breaking [4,5]. In particular, Lee *et al* [5] emphasised the importance of non-Bragg scattering mechanisms in explaining Doppler spectra at low grazing angles. A particular technical problem that needs to be addressed is that the tail of the Doppler spectra tend to be highly variable (spiky), which has a significant effect on CFAR processing for detecting low RCS targets that appear in the Doppler clutter band.

Attempts have been made to create models of low grazing angle Doppler spectra based on an analysis of the Doppler lineshape [5,6]. This project uses two Gaussians to fit the fast and slow Doppler components of the spectrum. A three stage approach has been adopted here. The scattering trends are examined, and so far the effects of grazing angle, radar frequency, radar bandwidth and wind speed have been investigated [7,8]. The variation of the Doppler spectra with the grazing angle of the radar and the radar frequency is discussed in detail here.

In the second stage of the project, a statistical model using the two Gaussian shapes, and based on the K-distribution type methodology, has been developed. The performance of this model has been

assessed and compared with data and other models [9-11]. Finally synthetic data have been generated using a Doppler memoryless non-linear transform (MNLT) [12]. Given the required spectral shape and Doppler bin statistics, simulated data can be generated that appear indistinguishable from real data.

Scattering Trends

The radar system used was MIDAS, which was built and operated by Racal (now called Thales). A single radar frequency could be selected out of a choice of 3, 10, 16, 35 and 94 GHz. The MIDAS radar was installed on a platform lift that could be raised and lowered to give different grazing angles to the water surface. 10 different grazing angles were used, between 3° and 24°, to collect data from 10 different wind-generated wave conditions and 8 mechanically generated wave conditions. The radar beamwidth was 5° at all the radar frequencies.

The speed of the wind generator is controllable, to give a maximum wind speed up to 12 ms⁻¹. This generates waves in the test-section, which can have a range of wavelengths from 10 cm to 75 cm. Larger waves can be generated in the wave tank using a mechanical wave maker.

Figure 1 shows the Doppler spectra at all the grazing angles collected for the 9.75 GHz radar frequency, and with a 12 ms⁻¹ wind speed in the wind tunnel. The spectra have been offset from each other to provide a waterfall plot on one graph. The grazing angle is shown next to each spectrum. The VV and HH superficially appear to change little as the grazing angle is varied, but in both cases, the velocity of the spectral peak decreases with the increasing grazing angle.

The HH spectra typically show an asymmetric Doppler peak with a longer

lower velocity tail, whereas the VV spectra are typically fairly symmetric. A Gaussian line-fitting routine has been applied to each spectrum. For VV a single broad Gaussian has been used, whereas in HH, each of the dotted lines is made up of the sum of two Gaussians that correspond to a 'slow' and a 'fast' component.

Fitting the Gaussian lineshapes is a convenient way of finding the peak of the Doppler spectra. The velocities of the components are shown in figure 2.

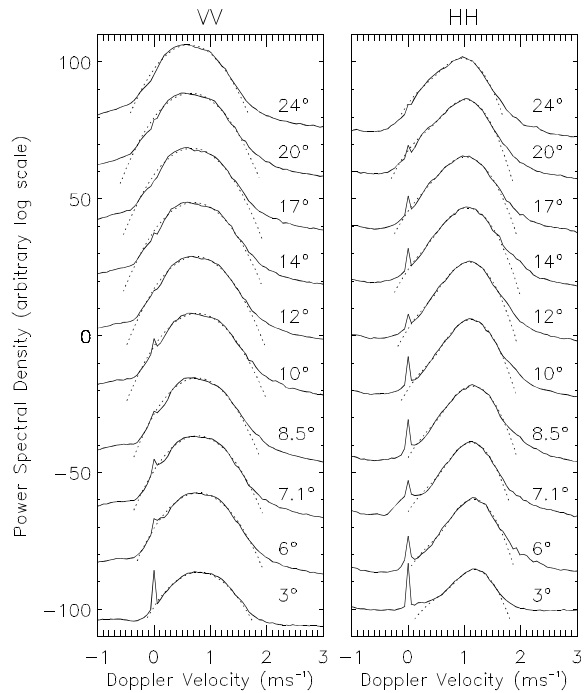


Figure 1: Doppler spectra collected using 9.75 GHz radar for different grazing angles. VV vertical, HH horizontal (transmit and receive).

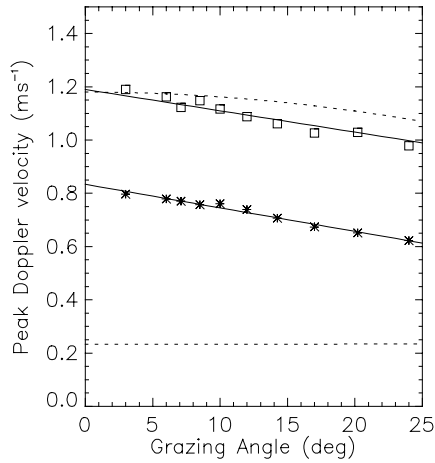


Figure 2: Variation in the velocity of the Doppler components shown in figure 1. Squares – fast component (HH). Asterisks – slow component (VV). The dotted line shows the approximate celerity of the wind waves in the radar line of sight and the phase velocity of the Bragg resonant ripples.

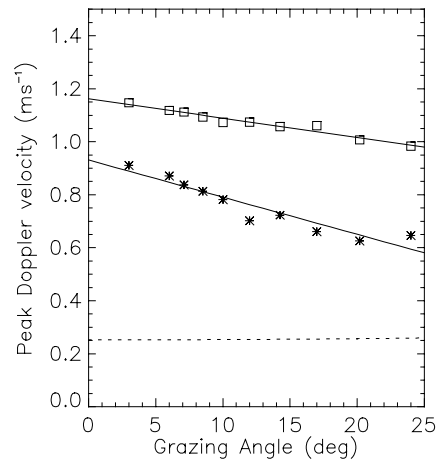


Figure 4: Variation in the velocity of the Doppler components for the 15.75 GHz radar data shown in figure 3. Squares – fast component (HH). Asterisks – slow component (VV). The dashed line shows the phase velocity of the Bragg-resonant waves at 15.75 GHz.

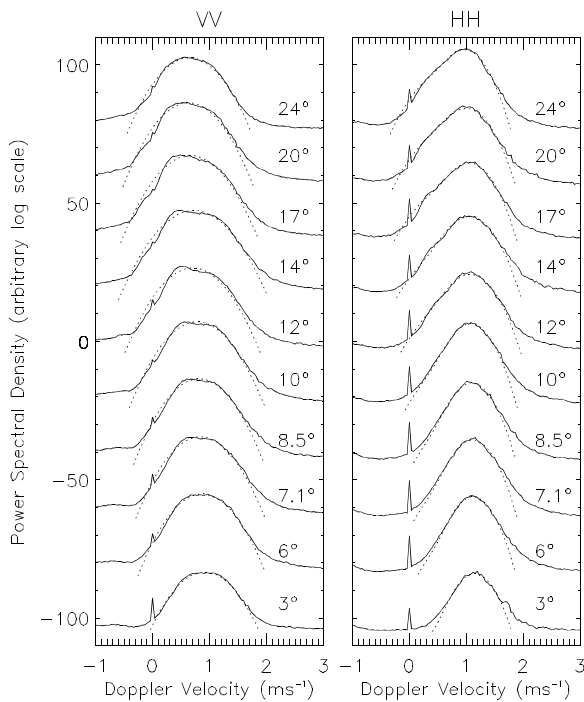


Figure 3: Doppler spectra collected using 15.75 GHz radar for different grazing angles. VV vertical, HH horizontal (transmit and receive).

The dotted line towards the bottom of the graph shows the expected velocity of the Bragg resonant gravity-capillary waves for that radar frequency. The orbital velocity of the larger dominant waves and the surface drift velocity in the wave tank was estimated to be around 0.35 ms^{-1} [13], but even with this contribution there would not be any agreement with the observed trend. This suggests that the observed scattering may be more complicated than simply Bragg scattering.

The celerity of the waves was around 1.18 ms^{-1} for the 12 ms^{-1} wind speed [8]. Wave celerity is the phase velocity of the waves in addition to the velocity caused by advection by the current in the wave tank. It might be expected that the velocity of the fast component would simply follow the component of the wave celerity in the radar line-of-sight, and so vary as $\cos(\theta)$, as shown by the dotted line at the top of the graph in figure 2. Instead, the fast scatter component falls off linearly with the

grazing angle. For this radar frequency, the velocity of both the slow and fast scatter component decreases at approximately the same rate.

Figures 3 and 4 were collected using the 15.75 GHz radar frequency. The VV data deviates somewhat from the simple picture of a single Gaussian with a somewhat more pronounced peak at lower velocity and a broad shoulder at higher velocity, but the overall trends in the position of the peaks are similar. Similar graphs of the velocity as a function of grazing angle have been found for radar frequencies of 3, 35 and 94 GHz respectively. For all five of the radar frequencies, the fast scatter component shows approximately the same velocity values for the different grazing angles, with a gradient, $dV/d\theta$, of $-0.008 \pm 0.001 \text{ ms}^{-1} \text{ deg}^{-1}$. This result was also reproduced for a number of other wind-wave conditions, where the gradient was unchanged, but the y-axis intercept at 0° changed with the celerity of the waves.

The slow scatter component has previously been identified with Bragg-resonant scatter [5,7], however the behaviour of the slow scatter component, shown here, is hard to reconcile with a Bragg-resonant scattering mechanism. The slow scatter component showed a linear relationship between the peak Doppler velocity and the grazing angle, like the fast scatter component. The gradients of the line and the intercepts, increased with increasing radar frequency and also with wind speed. The influence of wave shadowing needs to be considered further, with the hope of explaining these results.

Statistical Modelling

An analytical model has been developed using K-distribution type methodology using 2 Gaussians as the starting basis [9]. Over short time periods, the mean frequency of the Gaussian lineshapes

fluctuates [11] and can be represented by a Gamma distribution [9,12]. For a single Gaussian, the moments of the spectrum may be evaluated as shown, and with a similar but more complicated result when both Gaussians are used.

$$\langle \hat{S}(\omega)^n \rangle = \frac{a^\alpha \sigma^{\alpha-n} \exp(-n\omega^2/2\sigma^2)}{\Gamma(\alpha)(2\pi)^{n/2} n^{\alpha/2}} 2^{\frac{\alpha-1}{2}} \frac{\Gamma(n+\nu)}{b^n \Gamma(\nu)} \times \left\{ \begin{array}{l} \Gamma(\alpha/2) {}_1F_1\left(\alpha/2, 1/2; \sigma^2(a-n\omega/\sigma^2)^2/2n\right) + \\ \sqrt{\frac{2}{n\sigma^2}} (n\omega - a\sigma^2) \Gamma((\alpha+1)/2) \times \\ {}_1F_1\left((\alpha+1)/2, 3/2; \sigma^2(a-n\omega/\sigma^2)^2/2n\right) \end{array} \right\}$$

$$\frac{1}{\nu(\omega)} = \frac{\langle S(\omega)^2 \rangle - \langle S(\omega) \rangle^2}{\langle S(\omega) \rangle^2}$$

Figure 5 and 6 shows an example spectrum and the corresponding spikiness of the data across the different spectral bins, as measured by the effective ν parameter. The $\nu(\omega)$ parameter is large (less spiky) in the Doppler bins around the spectral peak and much more spiky out in the tails of the spectrum, as is typical for data.

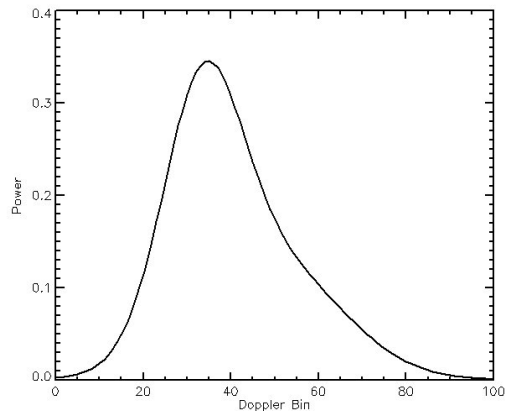


Figure 5: Doppler spectrum using statistical model.

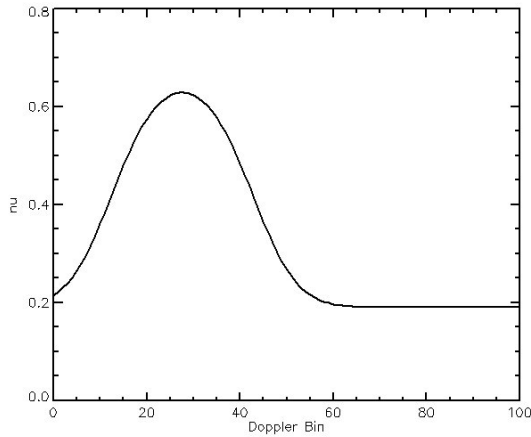


Figure 6: ν parameter (spikiness) versus Doppler bin.

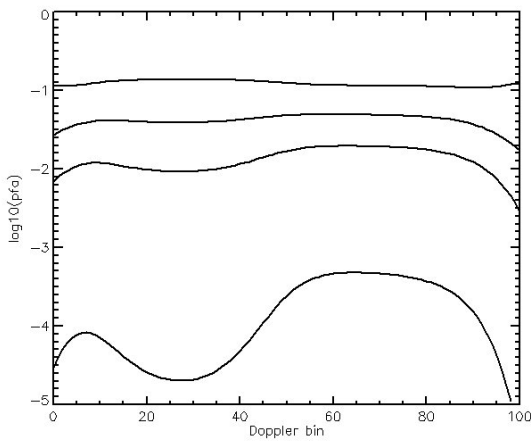


Figure 7: probability of false alarm versus Doppler bin for four different thresholds.

A small amount of thermal noise was added to the model before calculating the Probability of false alarm curves (P_{fa}) shown in figure 7. Otherwise the P_{fa} does not drop away, even completely outside the clutter spectrum. The model shows higher P_{fa} values in the tail of the spectrum that is in good qualitative agreement with real radar data. A detailed comparison of pulse Doppler radar detection performance in sea clutter, using data and other models has been performed [10].

Simulations

An elegant approach based on a Memoryless Non-Linear Transform (MNL) method has been developed that generates time correlated K-distributed data [12]. Previous models for sea clutter do not incorporate both the Doppler spectrum and amplitude distributions simultaneously and typically do not consider time dependence and temporal correlation, as this model does.

The model developed here requires three input pieces of information:

- the time-averaged Doppler power, $S(\omega)$, of the clutter (as a function of frequency)
- the time-averaged Gamma shape, $\nu(\omega)$
- the correlation time, τ .

Figure 8 shows a comparison of multi-band pulse radar data from Sennen Cove, with simulated data that has the same values of $S(\omega)$, $\nu(\omega)$ and τ [12].

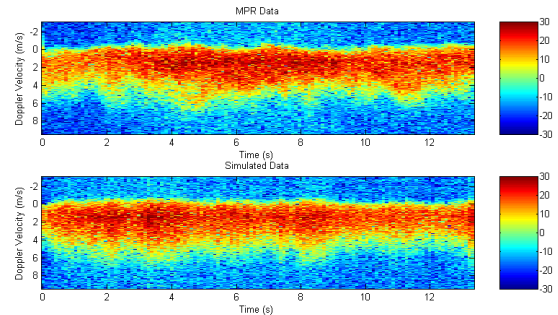


Figure 8: Comparison of real and simulated Doppler spectrograms.

Future Work

The trends in the data examined so far have concentrated on the radar parameters. The effect of environmental factors such as the wind speed, sea state and look direction relative to the wind will be examined in future, in order to develop a predictive capability for modelling coherent sea clutter.

Development of the statistical model will continue and the model will be applied to

the assessment of coherent signal processing methods. Once a robust model has been developed, which is shown to be widely applicable to real clutter, then potential improvements in radar signal processing design may be addressed.

References

1. CROMBIE D. D., 'Doppler spectrum of sea echo at 13.56Mc/s', *Nature*, 1955, **175**, pp681-682
2. PIDGEON V. W., 'Doppler dependence of radar sea return', *J. Geophys. Res.*, 1968, **73**, pp1333-41
3. PLANT W. J., 'A model for microwave Doppler sea return at high incidence angles: Bragg scattering from bound, tilted waves', *J. Geophys. Res.*, 1997, **102**, (C9), pp21131-21146
4. FUCHS J., REGAS D., WASEDA T., WELCH S., and TULIN M. P., 'Correlation of hydrodynamic features with LGA radar backscatter from breaking waves', *IEEE Trans. Geosci. Remote Sens.*, 1999, **37**, (5), pp2442-2460
5. LEE P. H. Y., BARTER J. D., BEACH K. L., CAPONI E., HINDMAN C. L., LAKE B. M., RUNGALDIER H. and SHELTON J. C., 'Power spectral lineshapes of microwave radiation backscattered from sea surfaces at low grazing angles', *IEE Proc. Radar, Sonar & Navig.*, 1995, **142**, (5), pp252-258
6. LEE P. H. Y., BARTER J. D., LAKE B. M. and THOMPSON H. R., 'Lineshape analysis of breaking-wave Doppler spectra', *IEE Proc. Radar, Sonar & Navig.*, 1998, **145**, (2), pp135-139
7. LAMONT-SMITH T., 'Investigation of the variability of Doppler spectra with grazing angle', DTC technical report, (submitted *IEE Proc. Radar, Sonar & Navig.*)
8. LAMONT-SMITH T., 'Variability of Doppler spectra with radar bandwidth',

DTC technical report

9. TOUGH R.J.A. and WARD K.D., 'Modelling of coherent radar sea clutter', DTC technical report
10. SHEPHERD P.W., TOUGH R.J.A. and WARD K.D., 'A comparison of pulse Doppler radar detection performance in sea clutter using data and models', DTC technical report
11. SHEPHERD P.W., TOUGH R.J.A. and WARD K.D., 'The short time behaviour of coherent sea clutter and its effect on radar performance', DTC technical report
12. GATES M.R., 'Simulation of coherent sea clutter', DTC technical report, (submitted to *IEE Radar 2004*)
13. LAMONT-SMITH T., FUCHS J. and TULIN M. P., 'Radar investigation of the structure of wind waves', *J. Oceanog.*, 2003, **59**, pp49-63

Acknowledgements

The analysis performed here was funded by EM Remote sensing Defence Technology Centre project (EMRS/DTC/1/18) with collaborating partners, MR Gates and J Branson of QinetiQ, Portsodwn West, and KD Ward, RJA Tough and PW Shepherd of TW Research.